Distribution Category:
LMFBR--Components: Base
Technology (UC-79k)

ANL-86-21



ARGONNE NATIONAL LABORATORY
9700 South Cass Avenue
Argonne, Illinois 60439

ANL--86-21

DE86 007852

# INSTABILITY CHARACTERISTICS OF FLUIDELASTIC INSTABILITY OF TUBE ROWS IN CROSSFLOW

by

S. S. Chen and J. A. Jendrzejczyk

Components Technology Division



April 1986

**CONTENTS**

## FIGURES

# INSTABILITY CHARACTERISTICS OF FLUIDELASTIC INSTABILITY OF TUBE ROWS IN CROSSFLOW

by

S. S. Chen and J. A. Jendrzejczyk

## ABSTRACT

An experimental study is reported to investigate the jump phenomenon in critical flow velocities for tube rows with different pitch-to-diameter ratios and the excited and intrinsic instabilities for a tube row with a pitch-to-diameter ratio of 1.75. The experimental data provide additional insights into the instability phenomena of tube arrays in crossflow.

## I. INTRODUCTION

Fluidelastic instability of tubes in crossflow has been studied extensively in the last 15 years. Several reviews of this problem are available .[1-3] The subject is continuing to receive more attention because of its significance in heat exchanger applications.

The general instability characteristics of different tube arrays are now fairly well understood. Of particular interest is the role of different fluid forces and different types of instability. It has been shown by Chen[4,5] that there are two types of fluidelastic instability: fluid-damping-controlled instability and fluid-stiffness-controlled instability. For a row of tubes, fluid-damping-controlled instability occurs at low mass-damping parameter ($\delta_m$), while fluid-stiffness-controlled instability occurs at high mass-damping parameter, and there is a discontinuity in the stability boundary at a certain value of $\delta_m$. In addition, at lower $\delta_m$, there are multiple stable and unstable regions. The first objective of this study is to investigate the "jump" in the critical flow velocity for tube rows with different pitch-to-diameter ratios.

There are two critical flow velocities for tubes conveying flow: intrinsic instability and excited instability.[6,7] A similar phenomenon has been noted for the instability of arrays in crossflow, but there is no detailed documentation of this characteristic. The second objective of this study is to investigate the difference of the two instability limits.

## II. TEST EQUIPMENT AND TEST PROCEDURES

The experiments are performed in a rectangular water channel, 10.7 cm (4.2 in.) wide and 25.9 cm (10.2 in.) high, of a test chamber connected to a water loop with a maximum flowrate of 0.052 $m^3/s$ (700 gpm). Tube rows are assembled in the channel; each tube element is suspended as a simply supported beam on two O-rings mounted 91.4 cm (36 in.) apart (see Fig. 1). The O-rings are seated in compression plates. The tube is submerged in fluid between the two O-ring supports (C1 to C2) but subjected to flow at the middle portion only. The overhang portion (C2 to C3) is in air. Note that tubes 1 and 5 are shorter to raise the natural frequencies.

Five brass tubes in a row are tested for four different pitch-to-diameter ratios (P/D): 1.35, 1.5, 1.6 and 1.75. The tube outside diameter is 1.59 cm (5/8 in.) and the tube wall thickness is 0.318 cm (1/8 in.). The nominal width of the water channel is 10.7 cm. However, the two walls can be shimmed to give proper spacing for different tube rows.

The instrumentation for each of the middle three tubes consists of two accelerometers mounted at the middle of the tube, oriented to be sensitive in the drag and lift directions. The accelerometers are installed by means of a small mounting block attached to the inside of the tubes and the leads brought to the outside.

A displacement transducer is located close to the free end of tube 4 to measure the displacement of tube 4 in the lift direction. When the tubes become unstable, they impact with one another; only the displacement transducer can provide useful information on tube response.

Tests for each tube row are made in still fluid and flowing fluid. Testing in still water is to determine the natural frequency and modal damping of each instrumented tube. The tube is excited by plucking it at the free end while the surrounding tubes are held at the overhang end by hand to prevent response of those tubes. The transient response of the tube is recorded. Then the damping is obtained from the log decrement of the acceleration trace, and the natural frequency is determined from the power spectrum of the acceleration. Each instrumented tube is tested in two orthogonal directions.

In flowing fluid, the flow velocity is increased at small intervals. At each flow velocity, the acceleration signals in the lift and drag directions are recorded on a magnetic tape for several minutes for subsequent analysis.

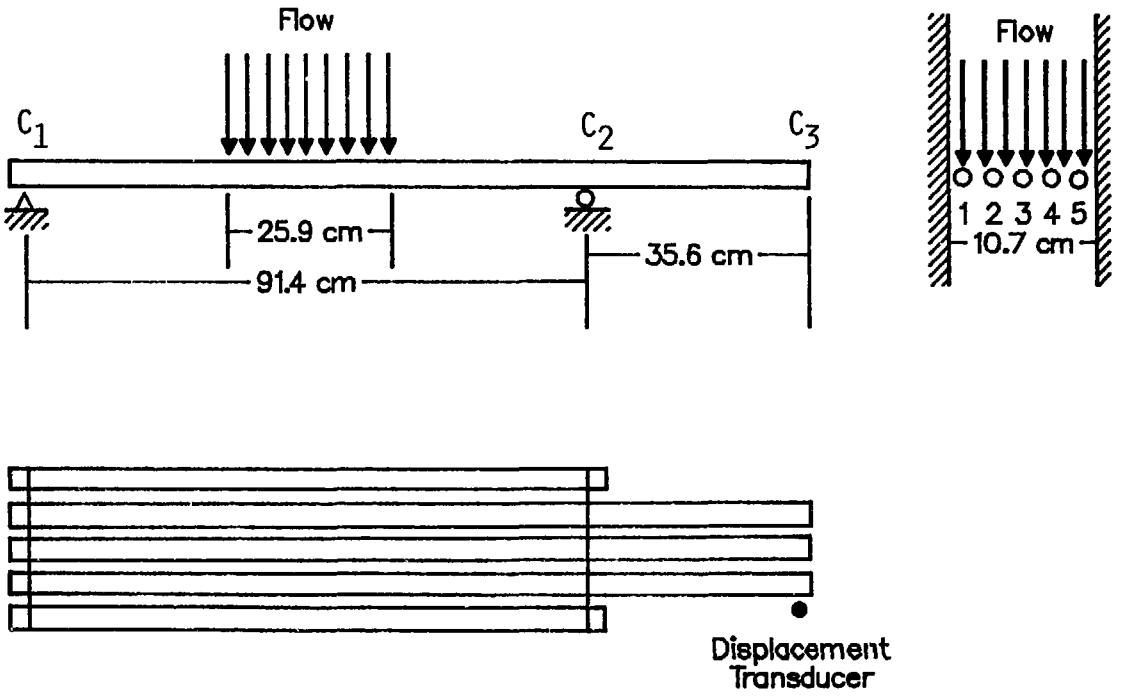


Fig. 1. Schematic of Tube Row

When appropriate, the flow velocity is increased very rapidly to reach the second stable region. Then, the flow is decreased at small intervals to determine the upper stability boundaries.

Critical flow velocity is a function of the initial disturbance.

• If the tubes are not excited with a mechanical excitation, the tubes lose stability by flutter spontaneously when the flow velocity is increased to a critical value; this flow velocity is called the critical flow velocity for intrinsic dynamic instability.

• If the tubes are excited by an external force, the tube may become unstable at a different flow velocity; this flow velocity is called the critical flow velocity for excited dynamic instability or induced dynamic instability.

The excited instability velocity is always smaller than the intrinsic instability velocity. The cricital flow velocities for both excited and intrinsic instability are determined relatively easily, as described below.

● Excited Instability Velocity: The velocity is increased at small intervals. For flow velocities smaller than the excited instability velocity, any motion of the tube caused by the transient disturbance to the tubes dies out. Once the flow is increased to the critical value the tube motion increases exponentially until it reaches the limit cycle.

● Intrinsic Instability Velocity: No mechanical excitation is given to the tubes. Once the flow velocity is increased to the critical value, large tube motion develops.

Tube damping depends on water temperature; this is attributed to O-rings, whose characteristics are a function of temperature. Therefore, tube damping can be controlled by controlling water temperature. In each tube row, the tubes were tested under several different temperatures.

## III. EXPERIMENTAL RESULTS AND DISCUSSION

Figures 2 and 3 show the natural frequency and modal damping ratio as functions of water temperatures for P/D = 1.5. Both natural frequency and modal damping ratio increased with decreasing water temperature. In all tube rows, fairly consistent results were obtained. The natural frequencies and damping for P/D = 1.35, 1.5 and 1.6 are similar. However, the values for P/D = 1.75 are higher, which can be attributed to the compression plates.

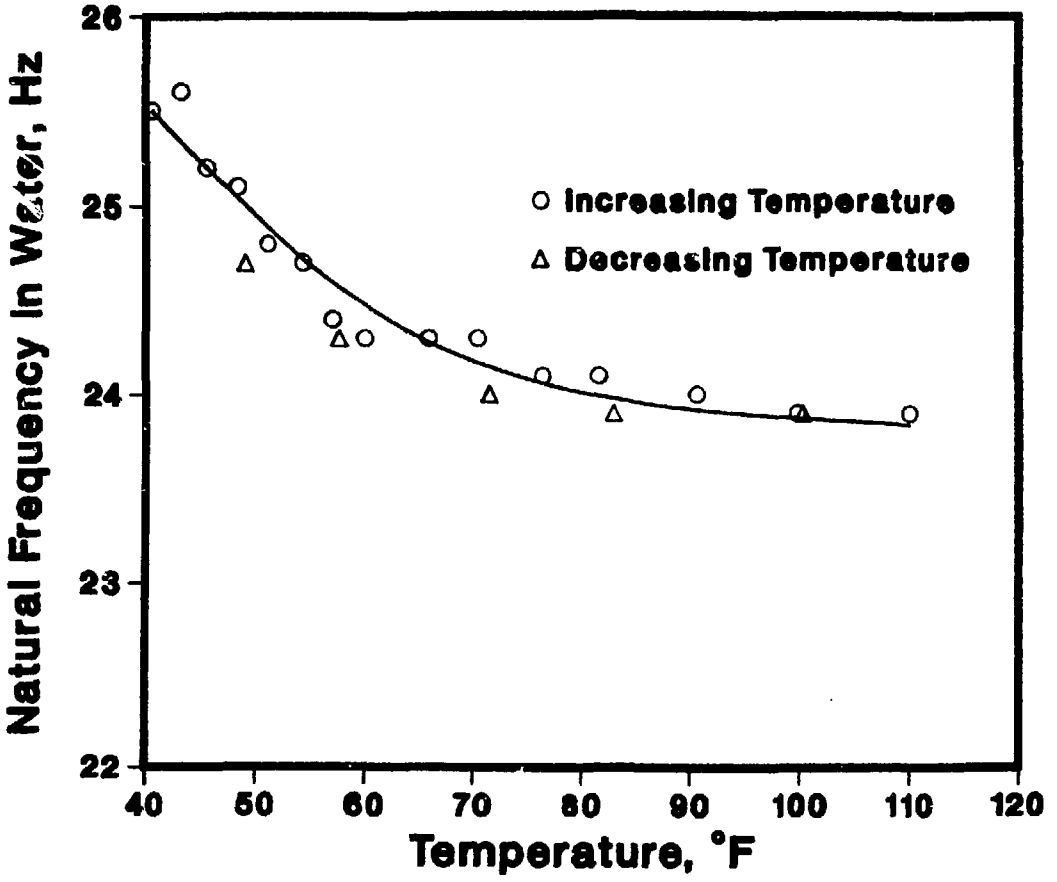


Fig. 2. Natural Frequencies in Water for P/D = 1.5

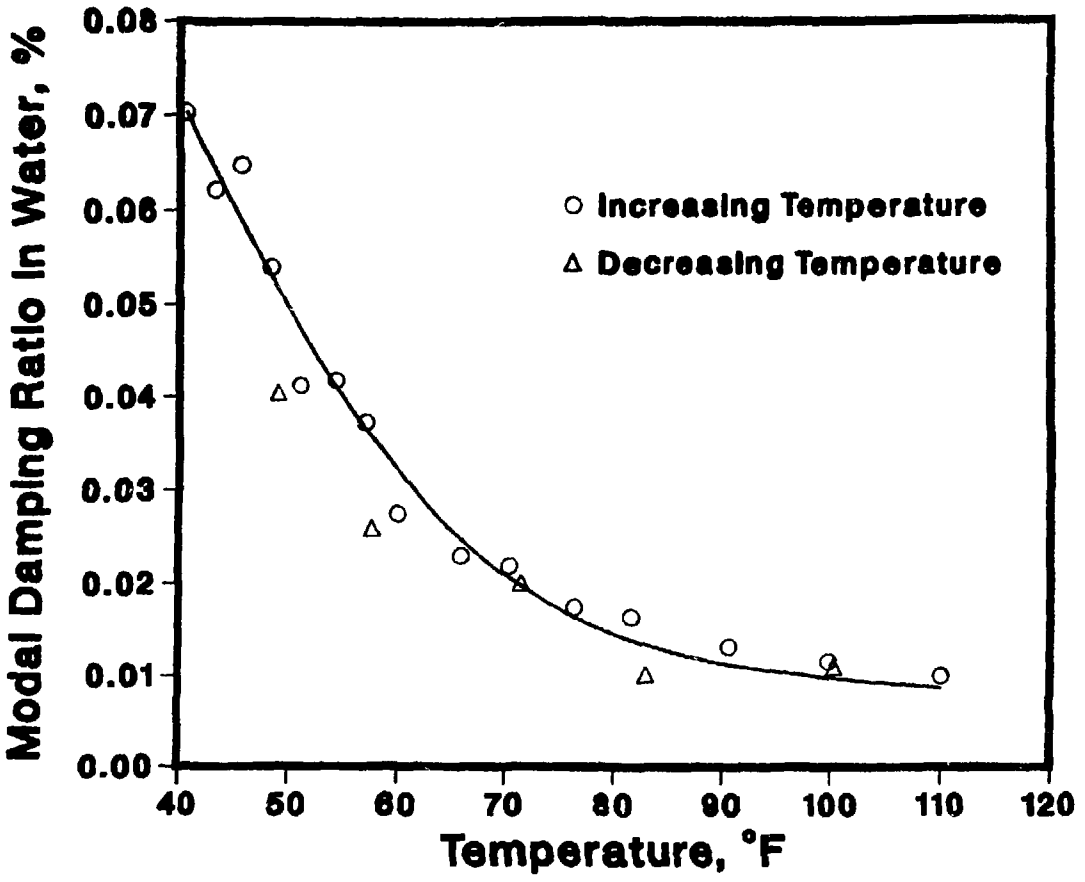


Fig. 3. Modal Damping Ratios in Water for P/D = 1.5

Tables 1 to 4 summarize results for the four tube rows, where $\rho$ is fluid density and D is tube diameter. The natural frequency (f) and modal damping ratio ($\zeta$) are those of an uncoupled mode in quiescent fluid. The flow with a uniform velocity U is acting on the middle portion of tube span. The mass (m) in the mass-damping parameter includes tube mass and added mass.

The stability boundaries are given in Fig. 4 for the four tube rows as a function of the mass-damping parameter $\delta_m$ ($= 2\pi\zeta m/\rho D^2$). Except for P/D = 1.75, the other three tube rows possess approximately the same damping values.

For P/D = 1.35, two instability boundaries are established.[8] For example, at $\delta_m = 1.0$, the tubes lose stability at $U_r$ ($= \frac{U}{fD}$) = 3.6 and regain stability at $U_r = 6.8$. In determining the lower stability boundary, the flow is increased gradually until instability develops. Once the tubes become unstable, tubes impact with one another. Theoretically, at $U_r = 6.8$, the tubes should regain stability. Practically, this is not the case, because of a nonlinear effect, which is discussed later. The upper stability limit is determined by rapidly increasing the flow to a value above the upper instability boundary, such that the tubes remain stable. Then the flow is decreased gradually. When it is reduced to the upper stability boundary, large tube oscillations occur. The buildup of large sinusoidal oscillations at the upper stability boundary is more rapid than at the lower one.

The discontinuity of stability boundary at a certain value of $\delta_m$ is demonstrated for two tube rows with P/D = 1.35 and 1.5. This discontinuous jump of the critical flow velocity is attributed to the transition from fluid-damping-controlled instability at low $\delta_m$ to fluid-stiffness-controlled instability at high $\delta_m$.[4,5] For P/D = 1.35, there is no fluid damping-controlled instability for $\delta_m > 1.5$, and the critical flow velocity jumps to a much large value associated with fluid-stiffness-controlled instability. For P/D = 1.5, the upper instability boundary cannot be determined experimentally. Before the flow can be increased to the upper stability limit, the tubes become unstable by the second mode; i.e., the critical flow velocity associated with the lower stability boundary of the second mode is smaller than the critical flow velocity associated with the upper stability boundary of the first mode. However, the discontinuous jump is identified. At $\delta_m = 1.75$, no instability of the tubes can be found for $U_r$ up to 9. Therefore, the jump occurs at $1.61 < \delta_m < 1.75$.

For P/D = 1.6 and 1.75, the values of $\delta_m$ at which the "jump" occurs lies outside the range of experiment. In these two cases, the jump cannot be determined.

Table 1. Experimental Data for P/D = 1.35

| Natural Frequency (f), Hz | Modal Damping Ratio ($\zeta$), % | Critical Flow Velocity, ft/s | $\frac{U}{fD}$ | $\frac{2\pi m\zeta}{\rho D^2}$ |
|---|---|---|---|---|
| 24.5 | 4.8 | 5.51<br>7.8 | 4.32<br>5.63 | 1.43 |
| 24.2 | 4.1 | 4.99<br>7.41 | 3.96<br>5.88 | 1.22 |
| 24.4 | 3.5 | 4.72<br>8.30 | 3.72<br>6.53 | 1.04 |
| 24.3 | 3.0 | 4.49<br>8.95 | 3.55<br>7.08 | 0.89 |
| 24.3 | 2.1 | 4.23<br>10.10 | 3.43<br>7.98 | 0.63 |
| 24.0 | 1.7 | 4.13<br>11.09 | 3.31<br>8.87 | 0.51 |
| 24.0 | 1.4 | 3.74 | 2.99 | 0.42 |

Table 2. Experimental Data for P/D = 1.5

| Natural Frequency (f), Hz | Modal Damping Ratio ($\zeta$), % | Critical Flow Velocity, ft/s | $\frac{U}{fD}$ | $\frac{2\pi m\zeta}{\rho D^2}$ |
|---|---|---|---|---|
| 25.1 | 5.4 | 7.60 | 5.81 | 1.61 |
| 25.0 | 5.0 | 6.93 | 5.32 | 1.48 |
| 24.6 | 3.4 | 6.06 | 4.70 | 1.02 |
| 24.6 | 3.1 | 5.53 | 4.31 | 0.91 |
| 24.1 | 2.0 | 4.97 | 3.95 | 0.60 |
| 24.0 | 1.5 | 4.72 | 3.78 | 0.44 |
| 23.9 | 1.1 | 4.63 | 3.72 | 0.34 |

Table 3. Experimental Data for P/D = 1.6

| Natural Frequency (f), Hz | Modal Damping Ratio ($\zeta$), % | Critical Flow Velocity, ft/s | $\frac{U}{fD}$ | $\frac{2\pi m\zeta}{\rho D^2}$ |
|---|---|---|---|---|
| 26.1 | 5.3 | 7.41 | 5.45 | 1.57 |
| 25.9 | 4.4 | 6.74 | 5.00 | 1.32 |
| 25.4 | 3.3 | 6.06 | 4.58 | 0.98 |
| 25.3 | 2.7 | 5.73 | 4.35 | 0.81 |
| 24.6 | 1.8 | 5.51 | 4.27 | 0.52 |
| 24.6 | 1.5 | 5.40 | 4.21 | 0.44 |
| 24.4 | 1.2 | 5.31 | 4.18 | 0.37 |
| 24.2 | 1.0 | 5.25 | 4.17 | 0.31 |

Table 4. Experimental Data for P/D = 1.75

| Natural Frequency (f), Hz | Modal Damping Ratio ($\zeta$), % | Critical Flow Velocity, ft/s | $\frac{U}{fD}$ | $\frac{2\pi m\zeta}{\rho D^2}$ |
|---|---|---|---|---|
| 27.7 | 10.8 | 9.80 | 6.79 | 3.22 |
| 27.6 | 10.2 | 9.67 | 6.73 | 3.04 |
| 27.5 | 9.5 | 9.51 | 6.64 | 2.82 |
| 27.5 | 9.0 | 9.21 | 6.43 | 2.67 |
| 27.4 | 8.2 | 8.90 | 6.23 | 2.45 |
| 27.2 | 7.2 | 8.51 | 6.00 | 2.13 |
| 27.1 | 6.4 | 8.03 | 5.70 | 1.90 |
| 26.9 | 5.8 | 7.58 | 5.41 | 1.72 |
| 26.6 | 5.0 | 7.42 | 5.36 | 1.49 |
| 26.4 | 4.6 | 6.88 | 5.00 | 1.37 |
| 26.3 | 4.5 | 6.92 | 5.05 | 1.34 |
| 26.1 | 4.2 | 6.87 | 5.05 | 1.25 |

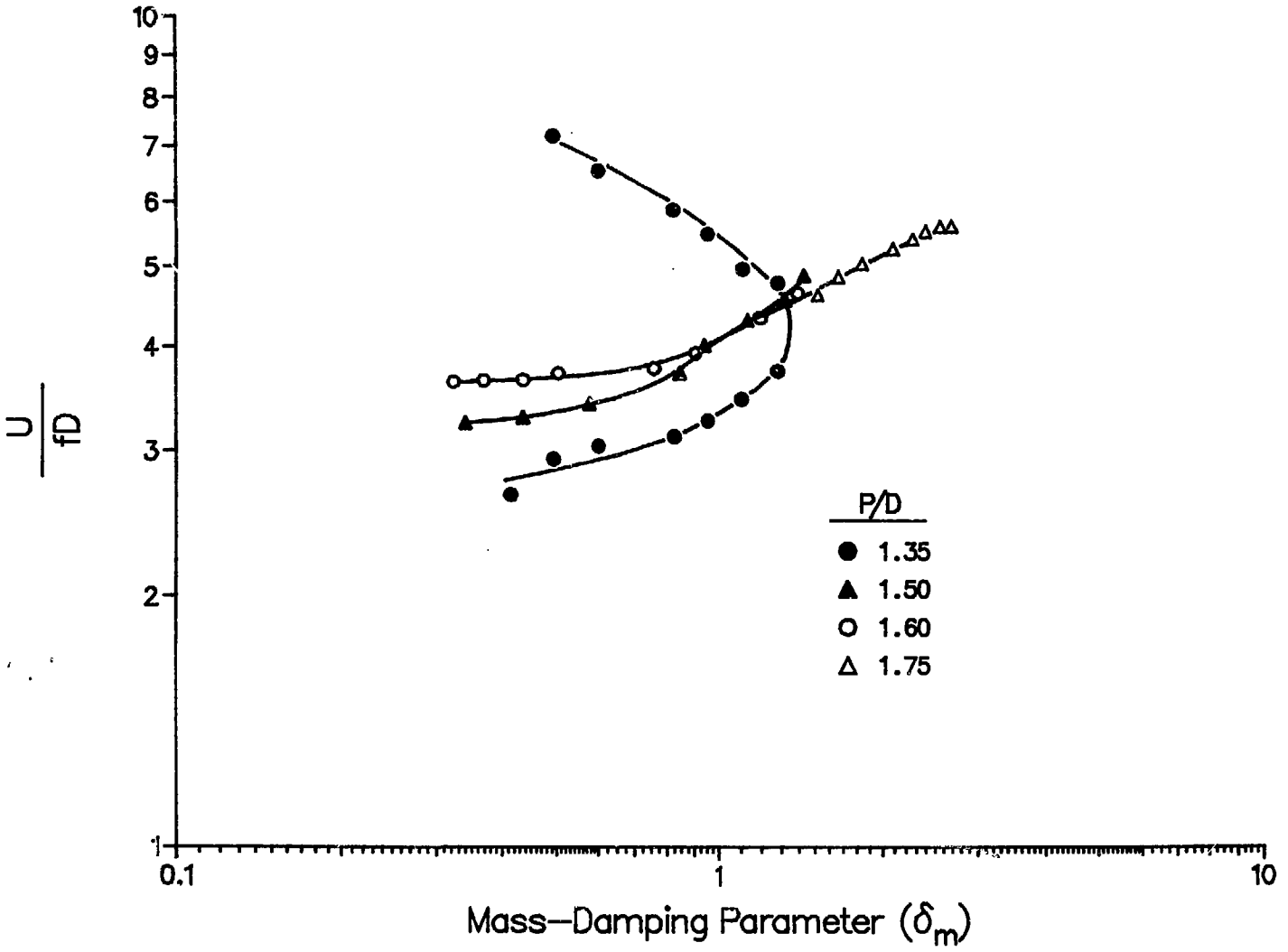


Fig. 4. Stability Boundaries for Four Tube Rows

Figure 4 shows that the critical flow velocities for fluid-damping-controlled instability depends on the pitch ratio P/D. As P/D increases, the lowest critical flow velocity increases.[5] This is the same as that for tube rows in air, in which the instablity is of fluid-stiffness-controlled type.[9] However, there is a significant difference.

The existence of multiple stable and unstable regions for tube rows at low $\delta_m$ can be examined using the fluid-damping coefficients. Theoretical and experimental results have illustrated that the lowest instability mode is associated with the tube motion in the lift direction. Consider a particular tube that is moving in the lift direction with a generalized displacement q while all other tubes are held rigid. The equation of motion is given as follows:[8]

$$\frac{dq^2}{dt^2} + 2\,\zeta\omega\,\frac{dq}{dt} + \omega^2 q = 0, \tag{1}$$

$$\zeta = \zeta_o(1 - c\,\dot{\alpha}_{11}) ,$$

where

$\omega$ is the circular frequency of oscillation, $\zeta_o$ is the modal damping ratio at $U_r = 0$, c is a parameter, which can be considered as a positive constant, and $\dot{\alpha}_{11}$ is the fluid-damping coefficient. For P/D = 1.33, $\dot{\alpha}_{11}$ is given in Fig. 5.

Equation 1 shows that the modal damping ratio depends on $\dot{\alpha}_{11}$, which in turn depends on $U_r$. Figure 6a shows a sketch of the variation of $\zeta$ with $U_r$ for several values of c ($c_1 > c_2 > c_3$). Note that, for $c\dot{\alpha}_{11} < 1$, the tube is stable and for $c\dot{\alpha}_{11} > 1$, it is unstable. The instability boundaries corresponding to $c = c_1$ and $c_2$ are also illustrated in Fig. 6b. For $c = c_3$, the tube is always stable. However, the modal damping decreases to a minimum at a certain value of $U_r$.

The variation of modal damping with flow velocity has been studied qualitatively for P/D = 1.35 and 1.5 for $\delta_m$ close to the jump area corresponding to $c = c_1$ and $c_3$ in Fig. 6a. The general trends are the same as those given in Fig. 6a.

The role of damping close to the jump area can also be demonstrated in Fig. 7. The accelerations of tube 2 in the lift direction are given in Fig. 7 at two values of $\delta_m$. At $\delta_m = 1.02$, which corresponds to $c = c_1$ in Fig. 6a, the tubes become unstable in the first mode. The instability builds up gradually. At $\delta_m = 1.80$, which corresponds to $c = c_3$ in Fig. 6a, the motion is small until $U \approx 8.55$ ft/s, when the tube becomes unstable by

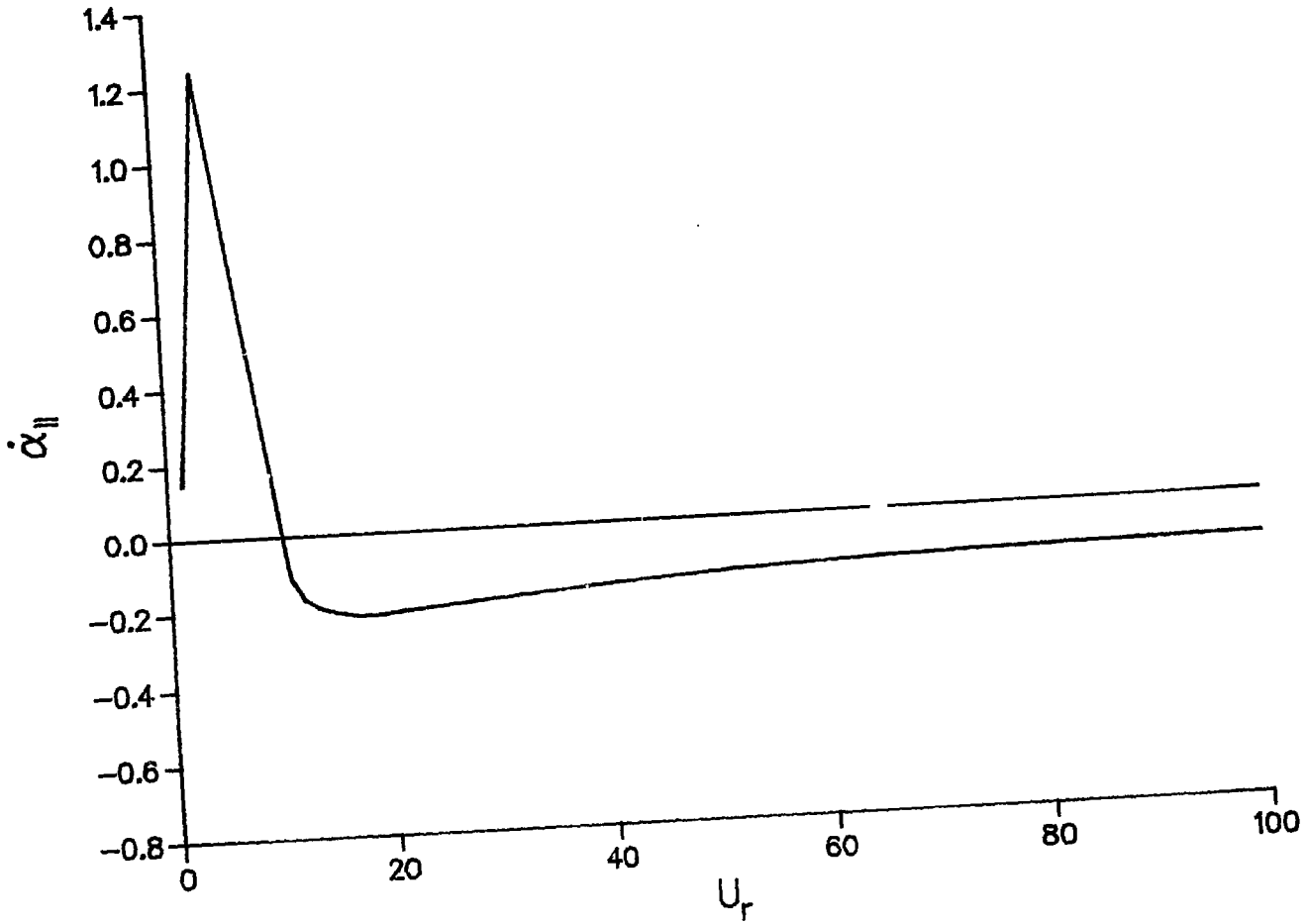


Fig. 5. Fluid-Damping Coefficient for P/D = 1.33

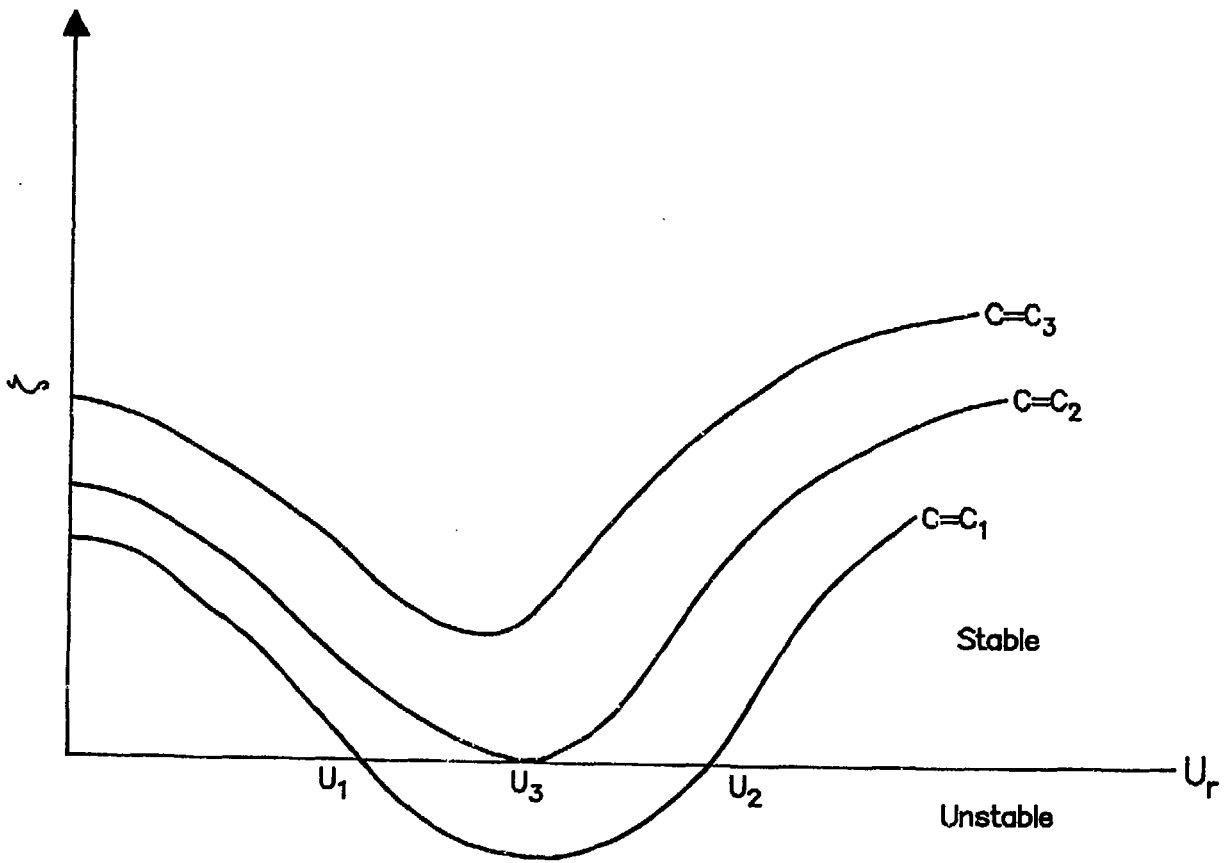


Fig. 6a. Sketch of Modal Damping Ratio

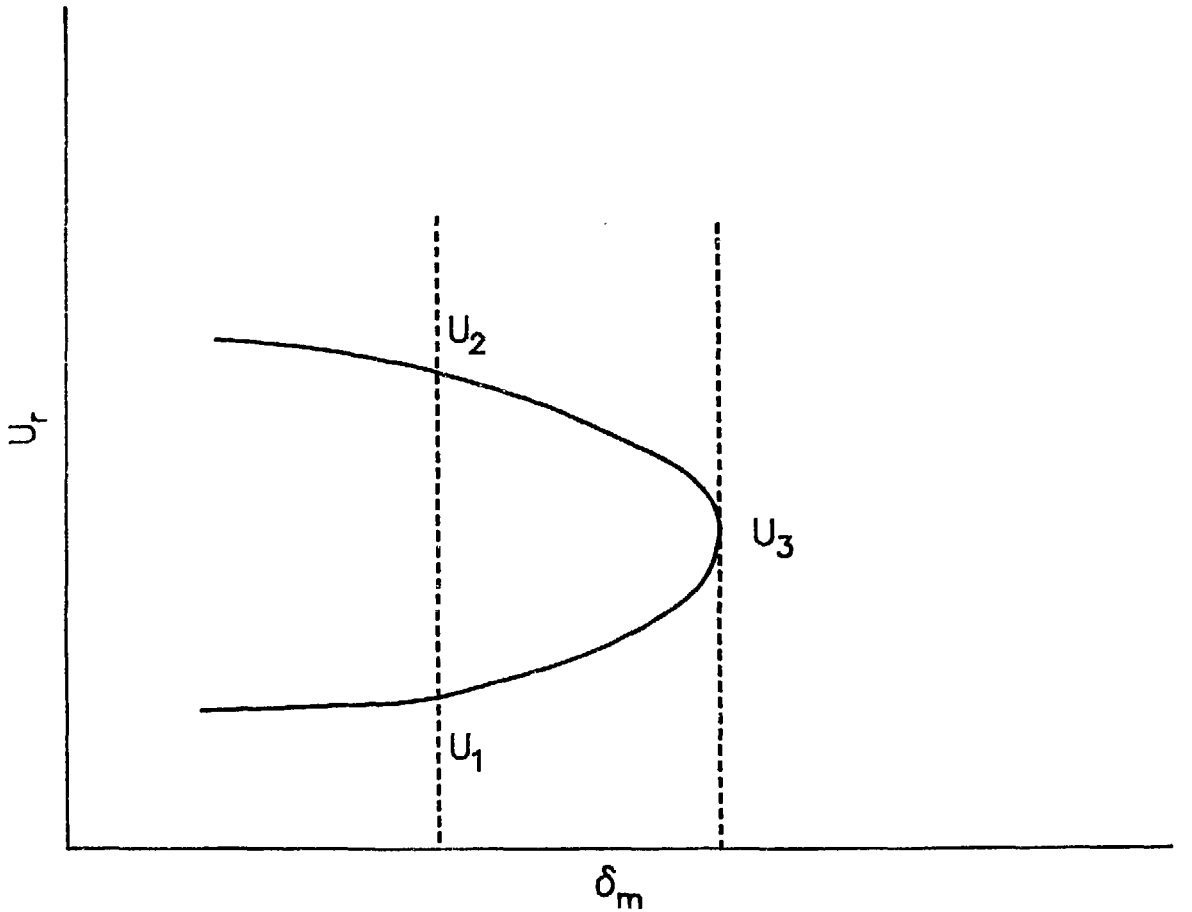


Fig. 6b. Sketch of Instability Boundaries

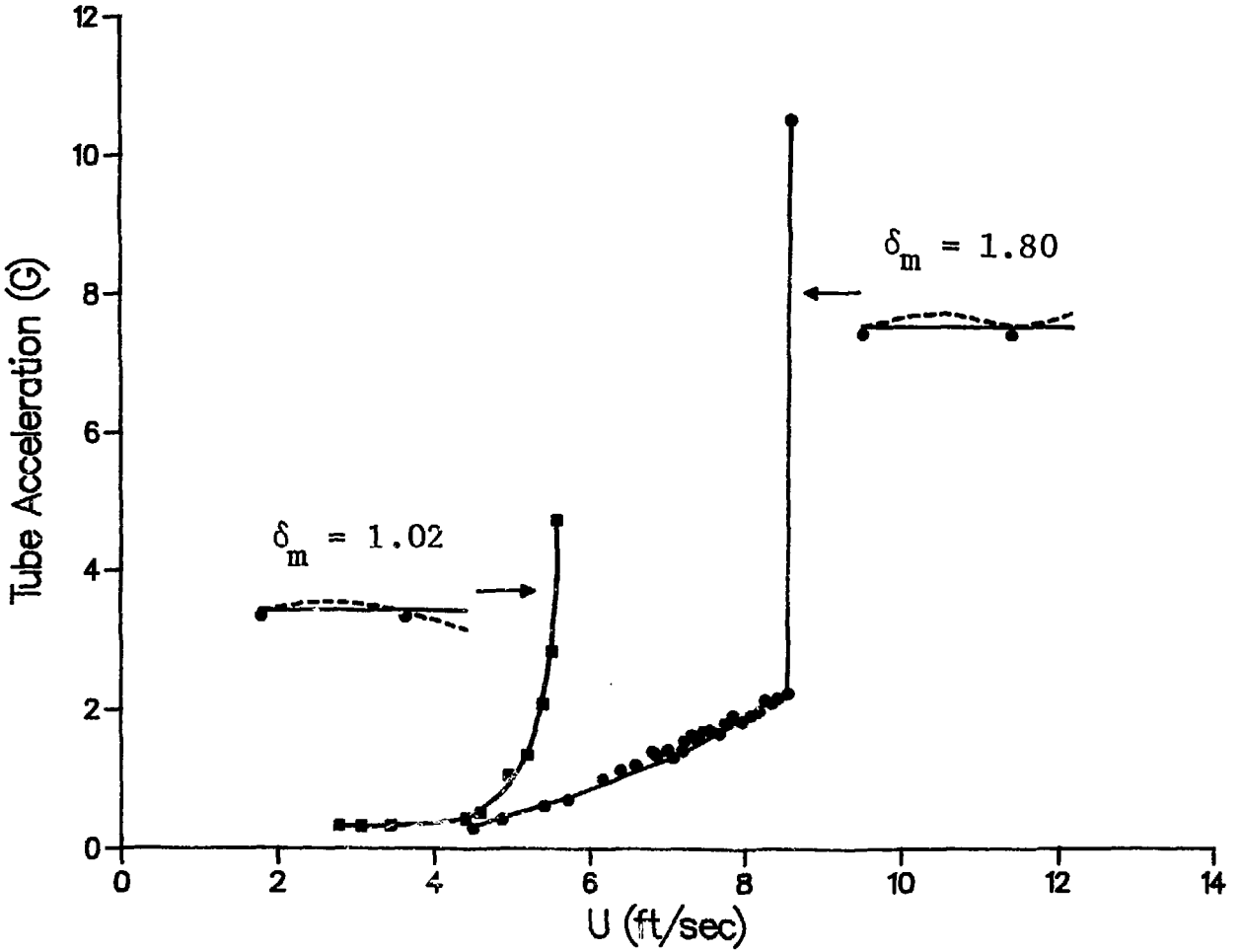


Fig. 7. Tube Accelerations for P/D = 1.5

the second mode. The instability of the second mode at $\delta_m = 1.80$ occurs spontaneously.

Although there are multiple stable and unstable regions and multiple critical velocities, in practical applications only the lowest critical flow velocity is important. Combining the experimental data for fluid-damping-controlled instability obtained in the tests and the data for fluid-stiffness-controlled instability by Ishigai et al.,[9] we can present the stability boundaries for P/D = 1.35, 1.5, and 1.75 in Fig. 8. Several general features are noted:

- There is a discontinuous jump in the critical flow velocity; the jump is attributed to the transition of two instability mechanisms.
- The critical flow velocity decreases with decreasing P/D.
- At high $\delta_m$ the critical flow velocity is proportional to $\delta_m^{0.5}$.
- The value of $\delta_m$ at which the jump occurs depends on P/D; the larger the value of P/D, the larger the value of $\delta_m$ for the transition point.

The critical flow velocity for fluid-stiffness-controlled instability obtained by Ishigai can be approximately expressed as follows:

$$\frac{U}{fD} = 5.55 \left(\frac{2\pi\zeta m}{\rho D^2}\right)^{0.5} \left(\frac{P}{D}\right)^{1.25} . \qquad (2)$$

The critical flow velocity is proportional to the half power of $\delta_m$ and 1.25 power of P/D for $1.19 \leq P/D \leq 2.68$.

In the past, hysteresis of tube response has been noted, but no detailed description of the phenomenon can be found in literature. A series of tests was performed for P/D = 1.75 to understand this phenomenon.

Figures 9 and 10 show two typical tube displacements with increasing and decreasing flow velocity at and near the instability boundary. Tube response follows different paths with increasing and decreasing flow velocity.

- Excited Instability: If the tubes are given proper mechanical excitation, the tubes may flutter in the excited instability region. Without mechanical excitations, the tubes are stable.

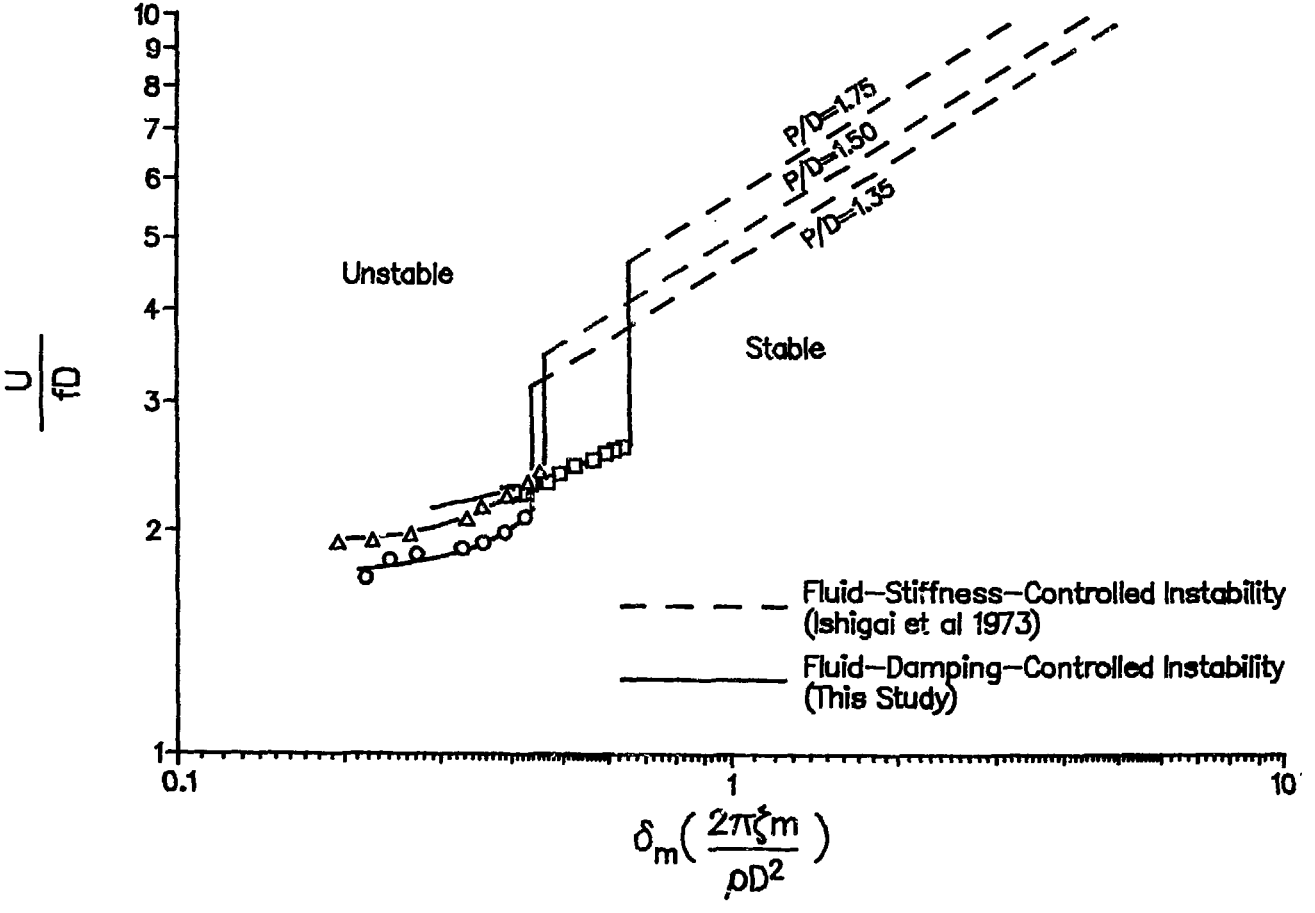


Fig. 8. Stability Map for Tube Rows

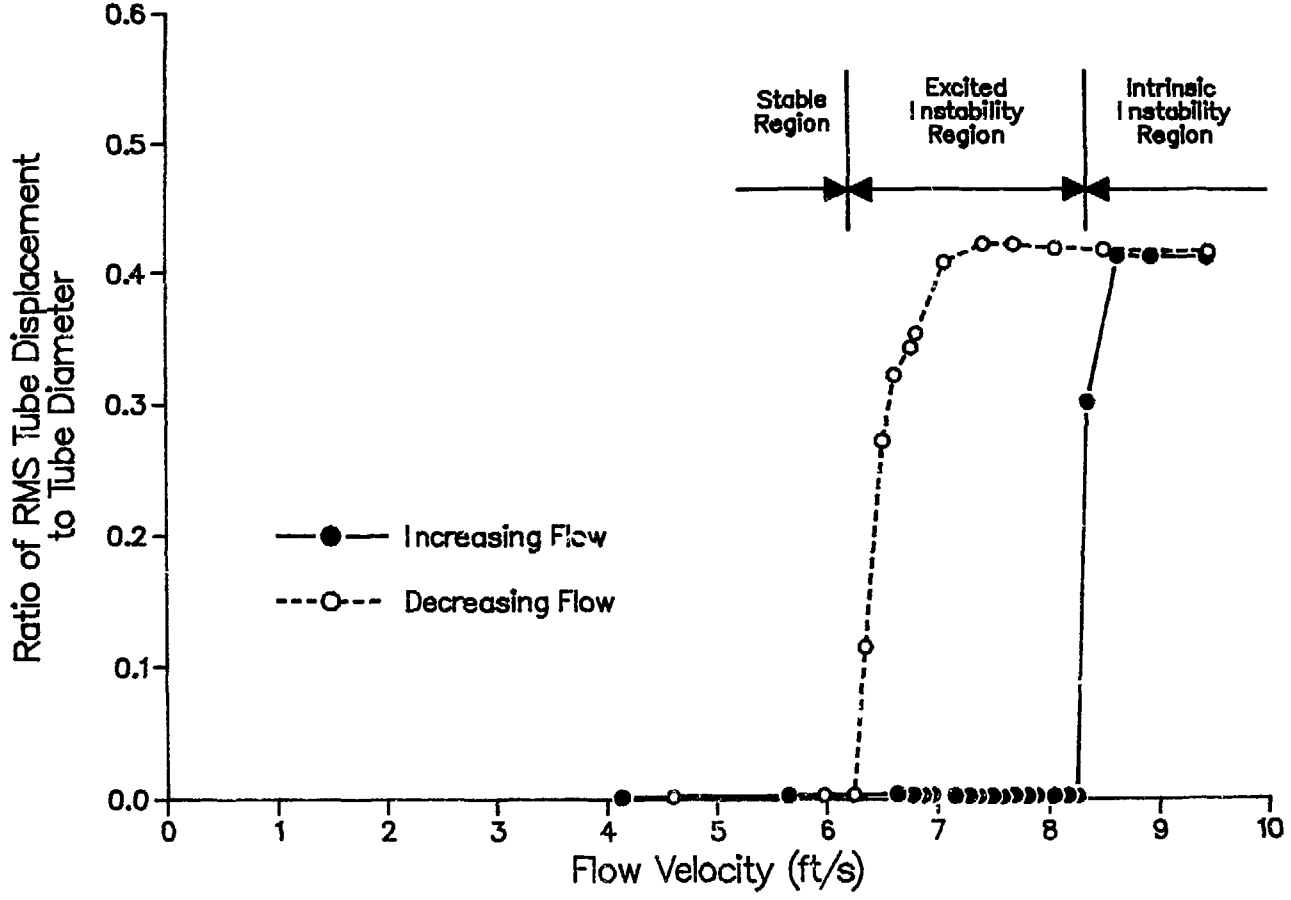


Fig. 9. Tube Displacement as a Function of Flow Velocity for P/D = 1.75 at $\delta_m$ = 2.15

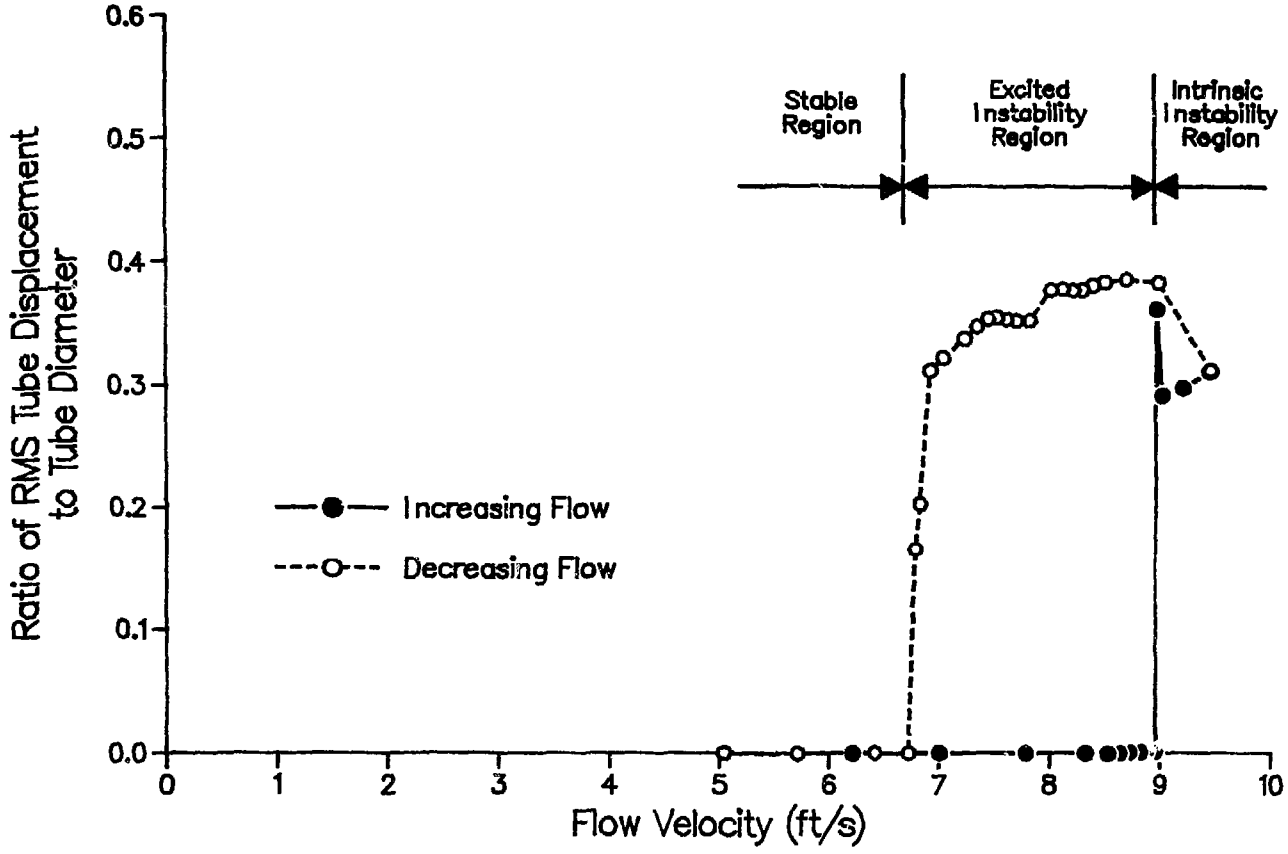


Fig. 10. Tube Displacement as a Function of Flow Velocity for P/D = 1.75 at $\delta_m = 3.25$

- Intrinsic Instability: No mechanical excitation is needed in this region. Once the flow is increased to the stability limit for intrinsic instability, large tube motion occurs.

Once the tubes lose stability either by intrinsic or excited instability, with decreasing flow large tube motion does not stop until the flow decreases to the lower limit of the excited instability region. The difference between the excited and intrinsic instability can be significant. For example, in Figs. 9 and 10, the intrinsic instability flow velocity is about 1.3 times the excited instability flow velocity.

Two types of excitations are applied to the tubes in the excited instability region at $\delta_m = 3.25$:

Excitation to a tube in the lift direction, and

Out-of-phase excitation to two neighboring tubes.

The results are summarized as follows:

U = 2.01 m/s (6.6 ft/s): The tubes are stable regardless of the excitations,

U = 2.10 m/s (6.9 ft/s): The tubes are stable with the first excitation and unstable with the second, and

U = 2.24 m/s (7.34 ft/s): The tubes are unstable with either excitation.

The excited instability flow velocity depends on the excitation. Therefore, the lowest critical flow velocity for excited instability is difficult to determine if there is a background mechanical excitation. The best way to determine its value is to increase the flow velocity to exceed the intrinsic critical flow velocity, then reduce the flow velocity slowly until large tube oscillations disappear. The lowest flow velocity at which large tube motion ceases is the lowest excited instability limit.

In the literature, only a single critical flow velocity is given; it is not known whether it is intrinsic or excited instability. This is one of the reasons that the critical flow velocities reported vary significantly among different investigators. In the examples of this test, the deviation can be as large as 30%.

There is another important implication for practical application related to the two types of instabilities. If the flow is accidentally increased to above the intrinsic instability speed and then is reduced to the excited instability region, large oscillations in the tubes will continue. This may damage equipment in a short time.

## IV. CLOSING REMARKS

In this report, four tube rows with different pitch-to-diameter ratios subjected to crossflow are tested to demonstrate instability features of fluidelastic instability. Specifically, the following characteristics are illustrated:

- There are two distinct instability mechanisms for tube rows in crossflow: fluid-damping-controlled instability and fluid-stiffness-controlled instability. The former is dominant for the low mass-damping values and the latter is dominant for the high mass-damping values.

- There is a discontinuous jump in the lowest critical flow velocity between the two instability regimes at a certain value of mass-damping parameter. The location of the jump depends on tube pitch.

- In the fluid-damping-controlled instability region, there are multiple stable and unstable regions. The controlling factor is the fluid-damping force associated with the motion of the tubes.

- At high $\delta_m$, the critical flow velocity is proportional to $\delta_m^{0.5}$, while at low $\delta_m$, it is not a linear function of $\delta_m^{0.5}$.

- Two instability flow velocities can be determined: excited instability and intrinsic instability. The excited instability flow velocity is lower than the intrinsic instability flow velocity. The difference between the two can be significant.

- The nonlinear effect of fluid force in the excited instability region is very important. Once the tubes become unstable, large tube motion will not cease until the flow is reduced to the lower limit of the excited instability region.

In the case of tube rows, the two instability mechanisms are clearly separated. However, in some other tube arrays, both fluid-damping and fluid-stiffness may be important simultaneously. Nevertheless, the general characteristics are not much different from the basic characteristics of tube rows.

## ACKNOWLEDGMENTS

This work was supported by the U.S. Department of Energy, Assistant Secretary for Nuclear Energy, Office of Reactor Systems, Development and Technology.

## REFERENCES


1. S. S. Chen, "Cross-Flow-Induced Instabilities of Circular Cylinders," The Shock and Vibration Digest 12(5), 21-34 (1980).

2. M. P. Paidoussis, "Flow-Induced Vibrations in Nuclear Reactors and Heat Exchangers: Practical Experiences and State of Knowledge," in Practical Experiences with Flow-Induced Vibrations, eds. E. Naudascher, and D. Rockwell, Springer-Verlag, Berlin, 1980, pp. 1-81.

3. S. S. Chen, "Instability of Circular Cylinder Arrays in Crossflow," The Shock and Vibration Digest 15(7), 17-26 (1983).

4. S. S. Chen, "Instability Mechanism and Stability Criteria of a Group of Circular Cylinders Subjected to Crossflow. Part I: Theory," J. of Vibration, Acoustics, Stress and Reliability in Design 105, 51-58 (1983).

5. S. S. Chen, "Instability Mechanism and Stability Criteria of a Group of Circular Cylinders Subjected to Crossflow. Part II: Numerical Results and Discussions," J. of Vibration, Acoustics, Stress and Reliability in Design 105, 253-260 (1983).

6. R. W. Gregory and M. P. Paidoussis, "Unstable Oscillation of Tubular Cantilevers Conveying Fluid: I. Theory, II. Experiment," Proc. Royal Soc. London 293(Series A), 512-542 (1966).

7. S. S. Chen and J. A. Jendrzejczyk, "General Characteristics, Transition, and Control of Instability of Tubes Conveying Fluid," J. Acoust. Soc. Am. 77(3), 887-895 (1985).

8. S. S. Chen and J. A. Jendrzejczyk, "Stability of Tube Arrays in Crossflow," Nucl. Eng. Des. 75(3), 351-374 (1983).

9. S. Ishigai, E. Nishikawa, and E. Yagi, "Structure of Gas Flow and Vibration in Tube Banks with Tube Axes Normal to Flow," Int. Symp. on Marine Eng., Tokyo, pp. 1-5-23 to 1-5-33 (1973).

## Distribution for ANL-86-21

Internal:

C. E. Till
R. S. Zeno
P. R. Huebotter
M. W. Wambsganss
S. S. Chen (10)
H. Halle
J. A. Jendrzejczyk (5)
T. M. Mulcahy
H. H. Chung
W. P. Lawrence
S. K. Zussman
R. A. Valentin
R. A. Lewis
Y. I. Chang
D. J. Malloy
R. W. Seidensticker
ANL Patent Dept.
ANL Contract File
ANL Libraries (2)
TIS Files (5)

External:

DOE-TIC, for distribution per UC-79k (114)
Manager, Chicago Operations Office, DOE
Director, Technology Management Div., DOE-CH
E. Gallagher, DOE-CH
Director, FFTF Project Office, U.S. DOE, Richland, WA
Manager, Engineering Technology Department, Foster Wheeler Energy Corp., Livingston, NJ (2)
M. K. Au-Yang, Babcock & Wilcox, Lynchburg, VA
E. B. Baumeister, Rocketdyne Div., Rockwell International, Canoga Park, CA
M. D. Bernstein, Foster Wheeler Energy Corp., Livingston, NJ
C. C. Bigelow, U.S. DOE/Nuclear Energy, Washington, DC
R. D. Blevins, GA Technologies Inc., San Diego, CA
J. C. Blomgren, Commonwealth Edison, Maywood, IL
G. J. Bohm, Westinghouse Electric Corp., Pittsburgh, PA
S. J. Brown, Quest Engineering and Development Corp., Houston, TX
C. C. Chamis, NASA - Lewis Research Center, Cleveland, OH
C. A. Chandley, Tennessee Valley Authority, Knoxville, TN
S. Chandra, Northeast Utilities Service Co., Hartford, CT
P. Y. Chen, U.S. NRC, Washington, DC
J. M. Chenoweth, Heat Transfer Research Inc., Alhambra, CA
H. J. Connors, Westinghouse Research & Development Center, Pittsburgh, PA
J. Corr, Saratoga, CA
W. K. Dahm, NASA, Marshall Space Flight Center, AL
A. Dalcher, General Electric Co., Sunnyvale, CA
E. H. Dowell, Duke Univ., Durham, NC
W. Edelstein, Illinois Institute of Technology, Chicago, IL
R. J. Fritz, General Electric Co., Knolls Atomic Power Laboratory, Schenectady, NY
E. L. Gluekler, General Electric Co., Sunnyvale, CA
O. K. Goetz, NASA, Marshall Space Flight Center, AL
N. Grossman, DOE/Nuclear Energy, Washington, DC
J. E. Haas, NASA - Lewis Research Center, Cleveland, OH
R. J. Hansen, Naval Research Laboratory, Washington, DC
M. Hartzmann, U.S. NRC/NRR, Washington, DC
R. A. Johnson, Rocketdyne Div., Rockwell International, Canoga Park, CA
S. P. Kalra, Electric Power Research Institute, Palo Alto, CA
E. Kiss, General Electric Co., San Jose, CA

B. T. Lubin, Combustion Engineering, Windsor, CT
K. McConnell, Iowa State U., Ames, IA
E. Moody, Rocketdyne Div., Rockwell International, Canoga Park, CA
R. J. Neuhold, U.S. DOE/Nuclear Energy, Washington, DC
E. H. Novendstern, Westinghouse Electric Corp., Pittsburgh, PA
E. E. Olich, General Electric Co., Sunnyvale, CA
P. R. Pluta, General Electric Co., Sunnyvale, CA
L. Povinelli, NASA - Lewis Research Center, Cleveland, OH
J. Rajan, U.S. NRC, Washington, DC
M. M. Reischmann, Office of Naval Research, Arlington, VA
E. L. Reiss, Northwestern Univ., Evanston, IL
B. J. Rock, U.S. DOE/Nuclear Energy, Washington, DC
J. A. Ryan, Hanford Engineering Development Lab., Richland, WA
J. B. Sandifer, Babcock & Wilcox Co., Alliance, OH
S. D. Savkar, General Electric Co., Schenectady, NY
M. Sax, Westinghouse - Bettis Atomic Power Laboratory, West Mifflin, PA
J. Schwab, NASA - Lewis Research Center, Cleveland, OH
J. C. Simonis, Southwest Research Institute, San Antonio, TX
N. R. Singleton, Westinghouse Electric Corp., Pittsburgh, PA
D. Steininger, Electric Power Research Institute, Palo Alto, CA
H. Struck, NASA - Marshall Space Flight Center, AL
M. R. Torres, General Electric Co., San Jose, CA
R. Volin, Shock & Vibration Information Center, Washington, DC
G. H. Weidenhamer, U.S. NRC/RES, Washington, DC
F. R. Wiltshire, General Electric Co., Sunnyvale, CA
T. M. Yang, General Electric Co., Sunnyvale, CA
E. A. Zanoni, Westinghouse - Bettis Atomic Power Laboratory, West Mifflin, PA

Components Technology Division Review Committee:
P. Alexander, Flopetrol Johnston Schlumberger, Houston, TX
D. J. Anthony, General Electric Co., San Jose, CA
A. A. Bishop, U. Pittsburgh, Pittsburgh, PA
B. A. Boley, Northwestern U., Evanston, IL
R. N. Christensen, Ohio State U., Columbus, OH
R. Cohen, Purdue U., West Lafayette, IN
R. E. Scholl, URS, San Francisco, CA
J. Weisman, U. Cincinnati, Cincinnati, OH

[redacted]

## TABLES